Available online at www.sciencedirect.com

ScienceDirect

Energy Procedia 55 (2014) 161 – 168

Energy Procedia

4th International Conference on Silicon Photovoltaics, SiliconPV 2014

A method to separate bulk lifetime and surface recombination velocity of silicon bricks based on transient photoluminescence

Kai Wang[a,]* and Henner Kampwerth[a]

[a]*School of Photovoltaic and Renewable Energy Engineering, University of New South Wales, Sydney 2052, Australia*

Abstract

We present a method to separate bulk lifetime and surface recombination velocity using transient photoluminescence (PL). With the use of the analytical expression of transient PL, the asymptotic separation of two transient PL decays excited by different wavelengths can be obtained. Combined with the use of the intensity ratio of two steady-state PL intensities excited by the two different wavelengths, the lifetime separation can be achieved. In addition, detailed methods to experimentally determine the two terms are presented.

Peer-review under responsibility of the scientific committee of the SiliconPV 2014 conference

Keywords: lifetime separation; silicon bricks; transient photoluminescence

1. Introduction

Photoluminescence (PL) is a powerful and fast tool for characterising silicon materials [1] and has been extensively used in characterising silicon wafers and bricks [2-9]. With the use of either steady-state [5, 6] or dynamic PL [7, 8], numerous methods have been proposed for separating surface and bulk lifetimes. In this paper, a method to achieve the lifetime separation with the use of two time-resolved PL decay measurements by different excitation wavelengths is proposed. This work could be regarded as an extension of our previous work on analytical solution of time-resolved PL from thick silicon wafers and bricks [9].

* Corresponding author. Tel.: +61430386572.
E-mail address: kai.wang@unsw.edu.au

Peer-review under responsibility of the scientific committee of the SiliconPV 2014 conference
doi:10.1016/j.egypro.2014.08.107

2. Theory

Figure 1 shows the situation to be analysed. We illuminate a silicon brick using a monochromatic light with wavelength λ_1 (absorption coefficient α_1) and measure PL at wavelength λ_2 (absorption coefficient α_2). If the recombination properties are assumed to be laterally uniform, we may use a one-dimensional model (along z direction) to study the excess minority carrier (hereafter "carrier" for simplicity) density as a function of depth into silicon and time. Furthermore, the expression of the transient PL signal can be obtained.

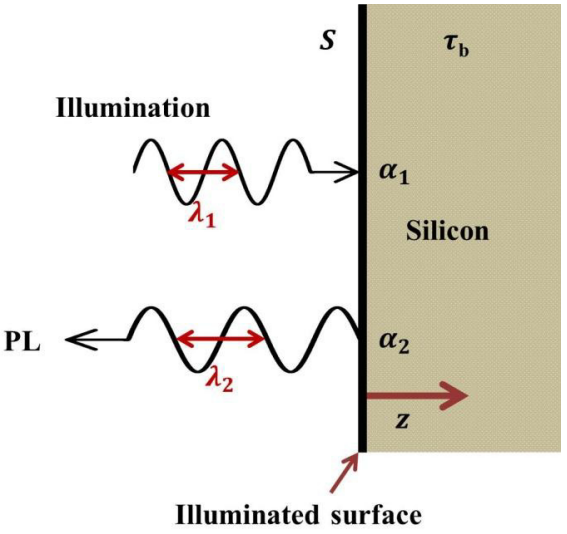

Fig. 1. A silicon brick is illuminated by monochromatic light with wavelength λ_1 (with absorption coefficient α_1). PL is subsequently measured at wavelength λ_2 (with absorption coefficient α_2).

All the carriers are assumed to be generated much farther than one carrier diffusion length away from the unilluminated surface, allowing us to take the brick as infinitely thick and to neglect the recombination properties of the unilluminated surface. The two recombination properties that need to be separated are therefore the bulk lifetime (τ_b) and the recombination velocity of the illuminated surface (S). From a mathematical perspective, two relations should be established between experimental measurements and two unknowns, τ_b and S. As mentioned by Buczkowski et al. in Ref. [10], there is a separation between two decay curves of the averaged carrier density for different excitation wavelengths (see Fig. 2 in Ref. [10]) and it increases with time and finally approaches its asymptotic value. For PL, there also exists a separation, δ, between two transient PL decays curves for different excitation wavelengths. As will be shown below, its asymptotic value, δ_a, is dependent on τ_b and S. We derive the expression for the transient PL decay in our previous work [9] and with slight improvement, the expression of δ_a can be obtained as a function of τ_b and S. In addition, the ratio of steady-state PL intensities excited by two different wavelengths is also dependent on τ_b and S. An additional advantage to use the ratio instead of absolute PL counts is that we can avoid the optical calibration constants. In a transient decay measurement, the illumination is assumed to be on for a sufficiently long time to allow the steady-state condition to build up, and is removed abruptly at $t = 0$. Therefore, the steady-state PL intensity is equal to the transient PL decay intensity when $t = 0$, allowing us to use two transient PL decay measurements excited by different wavelengths to experimentally determine the asymptotic separation as well as the intensity ratio.

Sections 2.1 and 2.2 will give the equations to describe PL for the steady-state and transient decay conditions. Section 2.3 elaborates how the steady-state PL intensity ratio and the asymptotic value of the separation are

determined from experimental measurements and Section 2.4 will present the algorithm used for lifetime separation in details.

2.1. Steady-state condition

Before studying the steady-state PL intensity, the steady-state carrier density needs to be determined. Under steady-state conditions, the continuity equation for a depth-dependent carrier density in a silicon brick, $\Delta n_{SS}(z)$, is given by [11]

$$D\frac{d^2\Delta n_{SS}(z)}{dz^2}-\frac{\Delta n_{SS}(z)}{\tau_b}+g(z)=0 \tag{1}$$

$$g(z)=\alpha_1 F\exp(-\alpha_1 z) \tag{2}$$

where D is the carrier diffusivity and F is the photon flux entering the silicon brick. $g(z)$ stands for the generation rate, which takes a simple exponential decay form.

The boundary condition at the illuminated surface is given by [11]

$$D\frac{d\Delta n_{SS}(z)}{dz}\bigg|_{z=0}=S\Delta n_{SS}(z)|_{z=0} \tag{3}$$

Combining Eqs. (1) to (3), we have

$$\Delta n_{SS}(z)=\frac{\alpha_1 F\tau_b}{\alpha_1^2 D\tau_b-1}\left(\frac{\alpha_1+\frac{S}{D}}{\frac{1}{\sqrt{D\tau_b}}+\frac{S}{D}}e^{-\frac{z}{\sqrt{D\tau_b}}}-e^{-\alpha_1 z}\right) \tag{4}$$

Taking reabsorption into consideration, the steady-state PL intensity is [12]

$$\begin{aligned}PL_{SS}(\alpha_1,\alpha_2,\tau_b,S)&=BB\left[1-R_f(\lambda_2)\right]\frac{N_A}{n_i^2}\alpha_2\int_0^\infty\Delta n_{SS}(z)e^{-\alpha_2 z}dz\\&=BB\left[1-R_f(\lambda_2)\right]\frac{N_A}{n_i^2}\alpha_2\frac{\alpha_1 F\tau_b}{\alpha_1^2 D\tau_b-1}\left(\frac{\alpha_1+\frac{S}{D}}{\frac{1}{\sqrt{D\tau_b}}+\frac{S}{D}}\frac{1}{\frac{1}{\sqrt{D\tau_b}}+\alpha_2}-\frac{1}{\alpha_1+\alpha_2}\right)\end{aligned} \tag{5}$$

where BB is the thermal radiation photon or energy flux emitted from the surface of a blackbody at the corresponding wavelength and temperature, N_A is the background doping density, n_i is the intrinsic carrier concentration and $R_f(\lambda_2)$ is the internal reflection of the detection wavelength at the front surface.

If two excitation wavelengths with absorption coefficients α_{11} and α_{12} are used, the intensity ratio of steady-state PL intensity can be expressed as

$$\varphi(\alpha_{11},\alpha_{12},\alpha_2,\tau_b,S)=\frac{PL_{SS}(\alpha_{11},\alpha_2,\tau_b,S)}{PL_{SS}(\alpha_{12},\alpha_2,\tau_b,S)}=\frac{\frac{\alpha_{11}}{\alpha_{11}^2D\tau_b-1}\left(\frac{\alpha_{11}+\frac{S}{D}}{\frac{1}{\sqrt{D\tau_b}}+\frac{S}{D}}\frac{1}{\frac{1}{\sqrt{D\tau_b}}+\alpha_2}-\frac{1}{\alpha_{11}+\alpha_2}\right)}{\frac{\alpha_{12}}{\alpha_{12}^2D\tau_b-1}\left(\frac{\alpha_{12}+\frac{S}{D}}{\frac{1}{\sqrt{D\tau_b}}+\frac{S}{D}}\frac{1}{\frac{1}{\sqrt{D\tau_b}}+\alpha_2}-\frac{1}{\alpha_{12}+\alpha_2}\right)} \tag{6}$$

2.2. Transient decay conditions

Similarly, the carrier density as a function of time and depth needs to be determined before studying the transient PL decay. Detailed procedures can be found in Ref. [9] and here we directly take the expression for the transient PL decay from Eq.(14) in Ref. [9]:

$$\begin{aligned}PL(\alpha_1,\alpha_2,\tau_b,S,t)&=BB\left[1-R_f(\lambda_2)\right]\frac{N_A}{n_i^2}\alpha_2\frac{\alpha_1FL^2}{D}\frac{1}{\sqrt{\pi}\sqrt{\frac{t}{\tau_b}}e^{\frac{t}{\tau_b}}}\\&\times\left[\frac{\left(\alpha_1L+\frac{SL}{D}\right)\left(\alpha_2L+\frac{SL}{D}\right)f\left(\sqrt{\frac{t}{\tau_b}}\right)}{\left(1-\frac{S^2L^2}{D^2}\right)(\alpha_1^2L^2-1)(\alpha_2^2L^2-1)}+\frac{\left(\alpha_1L+\frac{SL}{D}\right)f\left(\alpha_2L\sqrt{\frac{t}{\tau_b}}\right)}{(\alpha_2^2L^2-1)(\alpha_2^2L^2-\alpha_1^2L^2)\left(\alpha_2L-\frac{SL}{D}\right)}\right.\\&\left.-\frac{\left(\alpha_2L+\frac{SL}{D}\right)f\left(\alpha_1L\sqrt{\frac{t}{\tau_b}}\right)}{(\alpha_1^2L^2-1)(\alpha_2^2L^2-\alpha_1^2L^2)\left(\alpha_1L-\frac{SL}{D}\right)}-\frac{f\left(\frac{SL}{D}\sqrt{\frac{t}{\tau_b}}\right)}{\left(\alpha_1L-\frac{SL}{D}\right)\left(\alpha_2L-\frac{SL}{D}\right)\left(1-\frac{S^2L^2}{D^2}\right)}\right]\end{aligned} \tag{7}$$

with the diffusion length $L=\sqrt{D\tau_b}$ and $f(\xi)=\sqrt{\pi}\xi e^{\xi^2}\mathrm{erfc}(\xi)$.

Let the transient PL decay intensity normalised to its steady-state value be defined as

$$PL_{norm}(\alpha_1,\alpha_2,\tau_b,S,t)=\frac{PL(\alpha_1,\alpha_2,\tau_b,S,t)}{PL(\alpha_1,\alpha_2,\tau_b,S,0)} \tag{8}$$

Therefore, the asymptotic separation of two normalised time-resolved PL decay curves is given by

$$\delta_a(\alpha_{11},\alpha_{12},\alpha_2,\tau_b,S) = \lim_{t\to\infty} \ln\left[\frac{PL_{norm}(\alpha_{11},\alpha_2,\tau_b,S,t)}{PL_{norm}(\alpha_{12},\alpha_2,\tau_b,S,t)}\right]$$

$$= \ln\Bigg(\Big(\Big(\alpha_{12}^2(\alpha_{11}+\alpha_2)(\alpha_{11}D+S)(\alpha_{11}^2D\tau_b-1)\Big(-S^2\tau_b\big(-1+(\alpha_{12}+\alpha_2)\sqrt{D\tau_b}\big)$$
$$+ D^2\tau_b\Big(\alpha_2^2+\alpha_{12}^2\big(1+\alpha_2S\tau_b-\alpha_2\sqrt{D\tau_b}\big)+\alpha_{12}\alpha_2\big(1+\alpha_2S\tau_b-\alpha_2\sqrt{D\tau_b}\big)\Big)$$
$$+ D\Big(-1+S\tau_b\big(\alpha_{12}+\alpha_2+\alpha_{12}\alpha_2S\tau_b-\alpha_{12}^2\sqrt{D\tau_b}-2\alpha_{12}\alpha_2\sqrt{D\tau_b}-\alpha_2^2\sqrt{D\tau_b}\big)\Big)\Big)\Big) \qquad (9)$$
$$/\Big(\alpha_{11}^2(\alpha_{12}+\alpha_2)(\alpha_{12}D+S)(\alpha_{12}^2D\tau_b-1)\Big(-S^2\tau_b\big(-1+(\alpha_{11}+\alpha_2)\sqrt{D\tau_b}\big)$$
$$+ D^2\tau_b\Big(\alpha_2^2+\alpha_{11}^2\big(1+\alpha_2S\tau_b-\alpha_2\sqrt{D\tau_b}\big)+\alpha_{11}\alpha_2\big(1+\alpha_2S\tau_b-\alpha_2\sqrt{D\tau_b}\big)\Big)$$
$$+ D\Big(-1+S\tau_b\big(\alpha_{11}+\alpha_2+\alpha_{11}\alpha_2S\tau_b-\alpha_{11}^2\sqrt{D\tau_b}-2\alpha_{11}\alpha_2\sqrt{D\tau_b}-\alpha_2^2\sqrt{D\tau_b}\big)\Big)\Big)\Big)\Big)\Bigg)$$

2.3. Determination of δ_a and φ from transient PL decay measurements

The two transient PL decays excited by different wavelengths are denoted as $PL_1(t)$ and $PL_2(t)$. Dividing $PL_1(t)$ by $PL_1(0)$ and $PL_2(t)$ by $PL_2(0)$, the normalised PL intensities denoted as $PL_{norm,1}(t)$ and $PL_{norm,2}(t)$ are as shown in Figure 3.

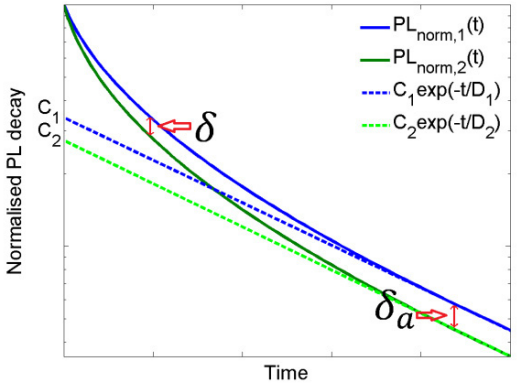

Fig. 2. Normalised time-resolved PL decay curves under excitation of two different wavelengths. The separation between two curves, δ, increases with time and reach its asymptotic value, δ_a. Two curves are fit by the approximation of $C_1 \cdot \exp(-t/D_1)$ and $C_2 \cdot \exp(-t/D_2)$ in order to experimentally determine δ_a with the minimum effect of noise.

Hypothetically, δ_a can be determined at $t \to \infty$

$$\delta_a = \lim_{t\to\infty} \ln\left[\frac{PL_{norm,1}(t)}{PL_{norm,2}(t)}\right] \qquad (10)$$

However, for transient PL decay measurements, the poor signal-to-noise ratio at large t would make the measurements unreliable, resulting in an erroneous measurement of $\delta_{a,exp}$. In order to minimise the effect of noise, the tail of $PL_{norm,1}(t)$ and $PL_{norm,2}(t)$ are fit by the approximation of $C_1 \cdot \exp(-t/D_1)$ and $C_2 \cdot \exp(-t/D_2)$, respectively. As the separation approaches its asymptotic value, D_1 should be equal to D_2. Therefore, we have

$$\delta_a = \lim_{t\to\infty} \ln\left[\frac{PL_{norm,1}(t)}{PL_{norm,2}(t)}\right] = \lim_{t\to\infty} \ln\left[\frac{C_1 \cdot \exp(-t/D_1)}{C_2 \cdot \exp(-t/D_2)}\right] = \ln\left(\frac{C_1}{C_2}\right) \tag{11}$$

φ can be obtained from the ratio of the initial PL intensities

$$\varphi = PL_1(0)/PL_2(0) \tag{12}$$

2.4. Separation algorithm

As shown in Eqs. (6) and (9), the two unknowns are τ_b and S. Therefore, by choosing appropriate values for α_{11}, α_{12} and α_2, we can map δ_a and φ over typical ranges of τ_b and S, as shown in Figure 3 (a) and (b).

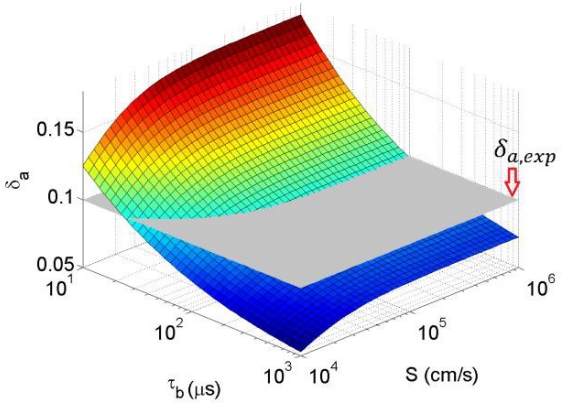

(a)

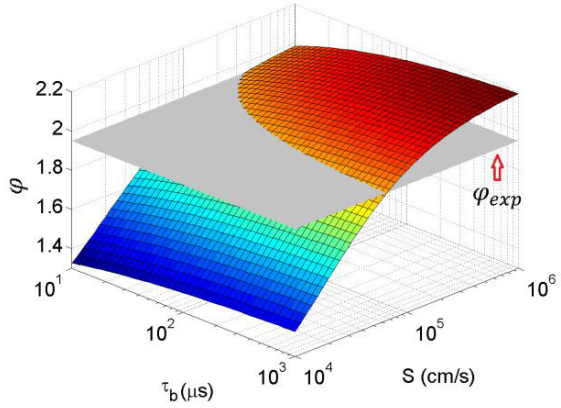

(b)

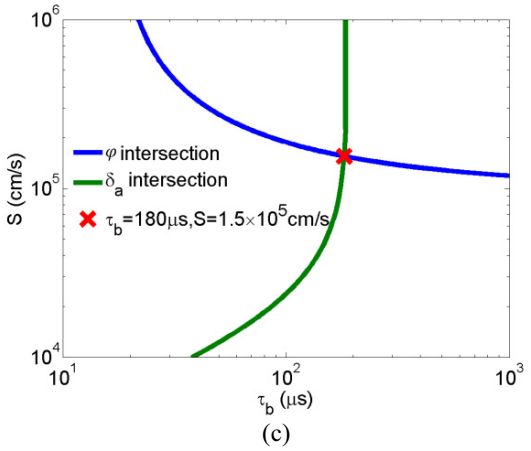

Fig. 3. (a) δ_a mapping and (b) φ mapping over typical ranges for τ_b and S, (c) intersection for lifetime separation. The two grey planes in (a) and (b) are used to intersect the mappings of δ_a and φ, yielding two curves as shown in (c). The intersection point of the two curves gives the values of τ_b and S. Parameters used for the calculation are: $\alpha_{11} = 272$ cm^{-1} (corresponding to an excitation wavelength of 910 nm [13]), $\alpha_{12} = 647$ cm^{-1} (corresponding to an excitation wavelength of 830 nm [13]), $\alpha_2 = 210$ cm^{-1}(corresponding to a detection wavelength of 930 nm [13]), $F = 2 \times 10^{17}$ cm^{-2}s^{-1} and $D_n = 26.92$ cm^2/s (corresponding to a p-type background doping density of $N_A = 1.5 \times 10^{16}$ cm^{-3} [14]).

Measurement of the two transient PL decays yields experimental values of δ_a and φ, denoted as $\delta_{a,exp}$ and φ_{exp}. The intersections of the calculated mappings of δ_a and φ using the planes specified by $\delta_a = \delta_{a,exp}$ and $\varphi = \varphi_{exp}$ yields two curves relating τ_b and S. Finally, the intersection of these two curves gives the separated values for τ_b and S, denoted as $\tau_{b,sep}$ and S_{sep}.

From a numerical perspective, we can define two deviation functions as in Eqs. (13) and (14):

$$DEV_1(\tau_b, S) = \left[\varphi(\tau_b, S) - \varphi_{exp}\right]^2 \tag{13}$$

$$DEV_2(\tau_b, S) = \left[\delta_a(\tau_b, S) - \delta_{a,exp}\right]^2 \tag{14}$$

Then, for a variety of τ_b, for example, τ_b ranging from 10 to 10^3 μs, DEV_1 and DEV_2 can be minimised by varying S. This can also be done by letting S range from 10^4 to 10^6 cm/s and minimising DEV_1 and DEV_2 by varying τ_b. Therefore, two relations between τ_b and S may be established. Furthermore, there exists only one pair of τ_b and S (the intersection point in Figure 3 (c)) that minimise DEV_1 and DEV_2 simultaneously and thus the lifetime separation is achieved.

Figure 3(c) shows an example of the lifetime separation algorithm. τ_b and S are taken to be 182 μs and 1.55×10^5 cm/s and other parameters are specified in the caption of Figure 3. Using Eq. (7), we could obtain two PL decay curves excited by different wavelengths. Using the procedure detailed in Section 2.3, we could get the experimental value of δ_a and φ as $\delta_{a,exp} = 8.86 \times 10^{-2}$ and $\varphi_{exp} = 2.05$. Intersecting the map of δ_a and φ using $\delta_{a,exp}$ and φ_{exp} (the two grey planes) in (a) and (b) would yield two curves relating τ_b and S as shown in (c). The intersection point of the two curves marked as "×" in (c), indicating that $\tau_{b,sep} \approx 180$ μs and $S_{sep} \approx 1.5 \times 10^5$ cm/s. Comparing the value of $\tau_{b,sep}$ with τ_b and S_{sep} with S, we could conclude that τ_b and S can be effectively separated using the algorithm proposed.

3. Summary

This paper proposed a method to separate the bulk and surface recombination properties of thick silicon wafers and bricks. Two time-resolved PL decay measurements must be conducted with different excitation wavelengths. The separation algorithm uses the analytical expressions of the ratio of two steady-state PL intensities as well as the

asymptotic separation of two time-resolved PL decay measurements. In addition, experimental methods of determining the intensity ratio and asymptotic separation are given by taking into consideration of the noise in real experiments. Finally, an example is given to prove that the proposed algorithm could effectively achieve the lifetime separation in details.

Acknowledgements

This Program has been supported by the Australian Government through the Australian Renewable Energy Agency (ARENA). Responsibility for the views, information or advice expressed herein is not accepted by the Australian Government.

References

[1] Trupke, T., Bardos, R. A., Schubert, M. C., Warta, W.. Photoluminescence imaging of silicon wafers. Applied Physics Letters, 89(4), 044107, 2006.
[2] Würfel, P., Trupke, T., Puzzer, T., Schäffer, E., Warta, W., Glunz, S. W.. Diffusion lengths of silicon solar cells from luminescence images. Journal of Applied Physics, 101(12), 123110, 2007.
[3] Macdonald, D., Tan, J., Trupke, T.. Imaging interstitial iron concentrations in boron-doped crystalline silicon using photoluminescence. Journal of Applied Physics, 103(7), 073710, 2008.
[4] Wang, K., McLean, W., Kampwerth, H.. Transient photoluminescence from silicon wafers: Finite element analysis. Journal of Applied Physics, 114(16), 163105, 2013.
[5] Mitchell, B., Trupke, T., Weber, J. W., Nyhus, J.. Bulk minority carrier lifetimes and doping of silicon bricks from photoluminescence intensity ratios. Journal of Applied Physics, 109(8), 083111, 2011.
[6] Giesecke, J. A., Kasemann, M., Schubert, M. C., Würfel, P., Warta, W.. Separation of local bulk and surface recombination in crystalline silicon from luminescence reabsorption. Progress in Photovoltaics: Research and Applications, 18(1), 10–19, 2010.
[7] Herlufsen, S., Ramspeck, K., Hinken, D., Schmidt, A., Müller, J., Bothe, K., Brendel, R.. Dynamic photoluminescence lifetime imaging for the characterisation of silicon wafers. Physica Status Solidi (RRL) - Rapid Research Letters, 5(1), 25–27, 2011.
[8] Giesecke, J. A., Sinton, R. A., Schubert, M. C., Riepe, S., Warta, W.. Determination of bulk Lifetime and surface recombination velocity of silicon ingots from dynamic photoluminescence. IEEE Journal of Photovoltaics, 3(4), 1311–1318, 2013.
[9] Wang, K., Green, M. A., Kampwerth, H.. Transient photoconductance and photoluminescence from thick silicon wafers and bricks: Analytical solutions. Solar Energy Materials and Solar Cells, 111, 189–192, 2013.
[10] Buczkowski, A., Radzimski, Z. J., Rozgonyi, G. A., Shimura, F.. Bulk and surface components of recombination lifetime based on a two-laser microwave reflection technique. Journal of Applied Physics, 69(9), 6495, 1991.
[11] Sze, S. M., Ng, K. K.. Physics of semiconductor devices. Hoboken, N.J.: Wiley-Interscience, 2007.
[12] Green, M. A.. Analytical expressions for spectral composition of band photoluminescence from silicon wafers and bricks. Applied Physics Letters, 99(13), 131112, 2011.
[13] Green, M. A., Keevers, M. J.. Optical properties of intrinsic silicon at 300 K. Progress in Photovoltaics: Research and Applications, 3(3), 189–192, 1995.
[14] Del Alamo, J., Swirhun, S., Swanson, R. M.. Measuring and modeling minority carrier transport in heavily doped silicon. Solid-State Electronics, 28(1-2), 47–54, 1985.